

Morphological relationship between axon and dendritic arborizations as revealed by Minkowski functionals

Marconi Soares Barbosa¹ and Luciano da Fontoura Costa¹

¹*Institute of Physics at São Carlos, University of São Paulo,
São Carlos, SP, PO Box 369, 13560-970, Phone +55 16 3373 9858,
FAX +55 162 71 3616, Brazil, marconi@if.sc.usp.br*

(Dated: December 7, 2021)

The spatial structure of the axonal and dendritic arborizations is closely related to the functionality of specific neurons or neuronal subsystems. The present work describes how multiscale Minkowski functionals can be used in order to characterize and compare the spatial organization of these two types of arborizations. The discrimination potential of the method is illustrated with respect to three classes of cortical neurons.

PACS numbers: 87.17.Nn, 87.57.Nk, 87.80.Pa, 89.75.-k

Human intelligence is to a great extent determined by the connectivity between the myriad of neuronal cells in the nervous system (Cajal:1989). Biologically, these connections are implemented by the *synapses* between neurons, which are strongly related to the shape of axons and dendrites (e.g. [1, 2, 3]). For instance, neural cells exhibiting more intricate dendritic or axonal arborizations tend to promote more connections. Therefore, the systematic study of the morphological properties of the axonal and dendritic trees can provide essential information about the connectivity of the nervous system. Because neurite outgrowth can be understood as a complex dynamical system involving pattern formation, biochemical regulation and electrical activity, they are particularly suitable for characterization and modeling by using concepts and methods from physics, computation and biology.

As the spatial distribution of synapses is to a great extent influenced by the interaction between the shape of dendrites and axons, and also because they share several developmental aspects, one question of particular relevance concerns the study to which extent these two types of structures are related (i.e. similar or distinct). Interestingly, both axons and dendrites start their lives as *neurites*, being differentiated during development. Along the early stages of neuronal growth, which involve many outgrowths and retractions, one of these neurites dominates and become the cell axon, assuming distinct biomolecular composition and function. In particular, axons seek actively for targets while being influenced by many trophic factors including differential adhesiveness, galvanotropism and chemotropism (e.g. [4, 5, 6]). Consequently, the shape of axons is directly affected by external field influences. At the same time, both dendrites and axons share intrinsic genetic and biochemical basis, which constrains neuronal growth and may imply intrinsic similarities between the dendritic and axonal arborizations of a same cell or category of cells. The current article addresses this important problem from the objective perspective of neuronal shape quantification by additive functionals [7], which have been previously applied with encouraging success to the characterization of dendritic

morphology (e.g. [8, 9]).

Integral geometry algorithms have been successfully used to characterize morphologically complex patterns and structures whose process of formation is not precisely known and is subject of modeling [7]. The central procedure is the calculation of intrinsic volumes or Minkowski functionals, a generalization of the usual determination of volume.

The Minkowski functionals of a body K in the plane are proportional to familiar geometric quantities, namely its area $A(K)$, perimeter $U(K)$ and the connectivity or Euler number $\chi(K)$. The usual definition of the connectivity from algebraic topology in two dimensions is the difference between the number of connected n_c components and the number of holes n_h , $\chi(K) = n_c - n_h$. In the Euclidean space, there is an additional geometric quantity, the mean curvature or breadth. Moreover there are two kinds of holes to consider: A pure hole, which is a completely closed region of white voxels surrounded by black pixels and tunnels. The Euler characteristic for the Euclidean space is then given by

$$\chi(K) = n_c - n_t + n_h, \quad (1)$$

where n_t is the number of tunnels and n_h is the number of pure holes. One instance where these functionals appear naturally is while attempting to describe the change in volume as the body K , now assumed to be convex, undergoes a dilation through a parallel set process using a ball B_r of radius r

$$V(K \oplus B_r) = V(K) + S(K)r + 2\pi B(K)r^2 + \frac{4\pi}{3}r^3. \quad (2)$$

Generalizing to higher dimensions, the change in hyper volume is given by the Steiner formula

$$v^d(K \oplus B_r) = \sum_{\nu=0}^d \binom{d}{\nu} W_\nu^{(d)}(K)r^\nu, \quad (3)$$

where the coefficients $W_\nu^{(d)}$ are referred to as Minkowski

functionals. For instance in the Euclidean space ($d = 3$),

$$\begin{aligned} W_0^{(3)}(K) &= V(K), & W_1^{(3)}(K) &= \frac{S(K)}{3}, \\ W_2^{(3)}(K) &= \frac{2\pi}{3}B(K), & W_3^{(3)}(K) &= \frac{4\pi}{3}\chi(K). \end{aligned} \quad (4)$$

Despite the wealth of results and continuum formulae for obtaining these functionals, it is useful to resource to the discrete nature of the binary images we wish to analyze by looking at the distribution of voxels in a Euclidean spatial lattice. By exploring the additivity of the Minkowski functionals their estimation resumes to counting the multiplicity of basic building blocks that disjointedly compose the object. The fundamental information needed here is a relationship for the functionals of an open interior of a n -dimensional body K which is embedded into a d -dimensional space

$$W_\nu^{(d)}(\check{K}) = (-1)^{d+n+\nu} W_\nu^{(d)}(K), \nu = 0, \dots, d. \quad (5)$$

With the absence of overlap between these building blocks and using the property of additivity of these functionals, we may write for a pattern \mathcal{P} composed of disjoint convex interior pieces \check{N}_m ,

$$W_\nu^{(d)}(\mathcal{P}) = \sum_m W_\nu^{(d)}(\check{N}_m) n_m(\mathcal{P}), \nu = 0, \dots, d, \quad (6)$$

where $n_m(\mathcal{P})$ stands for the number of building elements of each type m occurring in the pattern \mathcal{P} . For the three-dimensional space we display in Table I the value of Minkowski functionals for the building elements in a orthogonal lattice of voxels. By using the information (with $a = 1$) presented in Table I and Equations (4), (5) and (6) we have

$$\begin{aligned} V &= n_3, & S &= -6n_3 + 2n_2, \\ 2B &= 3n_3 - 2n_2 + n_1, & \chi &= -n_3 + n_2 - n_1 + n_0, \end{aligned} \quad (7)$$

Where n_3 is the number of interior cubes, n_2 is the number of open faces, n_1 is the number of sides and n_0 is the number of vertices. So the procedure to calculate Minkowski functionals of a pattern \mathcal{P} has been reduced to the proper counting of the number of elementary bodies of each type that compose a voxel (cubes, faces, edges and vertexes) involved in the make up of \mathcal{P} .

m	\check{N}_m	$W_0^{(3)}$	$W_1^{(3)}$	$W_2^{(3)}$	$W_3^{(3)}$
0	\check{V}	0	0	0	1
1	\check{L}	0	0	1/2	1
2	\check{F}	0	2	1	1
3	\check{C}	1	6	3/2	1

TABLE I: Minkowski functionals $\mathcal{M}_\nu^{(3)}$ for open elementary open sets \check{N}_m which compose a voxel K (of side $a = 1$): \check{V} (vertex), \check{L} (side), \check{F} (face) e \check{C} (cube).

The recent effort aimed at replicating a working micro column of cortex tissue [10] has motivated the dissemination of comprehensive data bases containing different anatomical classes of neuronal cells. We have considered several neuroLucida data from anatomically different types of cells, namely the anatomical classes MC1, BTC and LBC that populate the cortex and are engaged in distinct functions in the working of a neocortical micro column. The morphological data was obtained from the Brain Mind Institute, EPFL database [11]. Exact dilations of both the axonal and dendritic trees were performed until the majority of holes and tunnels disappeared, i.e., when the Euler number approaches 1. This implied a total number of 1000 dilations. All four Minkowski functionals were calculated along such dilations, so as to obtain a morphological signature for the dendritic and axonal arborizations of each cell. We then conducted a morphological analysis using a subset those values at selected scales, namely after 1,250, 500, 750 and 1000 exact dilation steps. In order to reduce the effect of the size of the cells on the measurements, the functionals were normalized respectively to the adequate power of the diameter of the cell, i.e the volume functional was normalized by L^3 , the surface area was normalized by L^2 and the mean-curvature was normalized by L . The Euler-number is a dimensionless topological measure and consequently did not undergo normalization. All measures were subsequently standardized, which is accomplished by subtracting the average and dividing by the standard deviation of each respective type of measurement (i.e. one of the 4 functionals). The standardized values therefore have zero means and unit variance, and most of their values are comprised between -2 and 2. Such a standardization reduces the influence of the overall relative magnitude of the different measurements.

The functionals were calculated separately for the dendritic and axonal trees of each neuron. For each case, the obtained measurements were organized into morphological vectors in the 20-dimensional space defined by the five spatial scales of each of the four functionals. Therefore, given a neuronal cell represented by their respective measurement vector, the morphological difference between its axon and dendritic arborizations can be quantified in terms of the magnitude μ of the vector corresponding to the difference between the respective feature vectors (i.e. axon and dendrites). Another important descriptor of the morphological space which has been considered in this work is the angle ϕ between the above difference vector and the vector which represents the mean of all such difference vectors. Such a measurement provides and indication of how much the axon-dendrite in each cell departs from the overall prototypical case (i.e. the average).

The result of the above procedure is presented in the scatterplot (i.e. the angle *versus* the magnitude of difference vectors for each neuron) in the composited Figure 1, which also shows the relative densities of the magnitudes of the difference vectors obtained by using a simple Gaus-

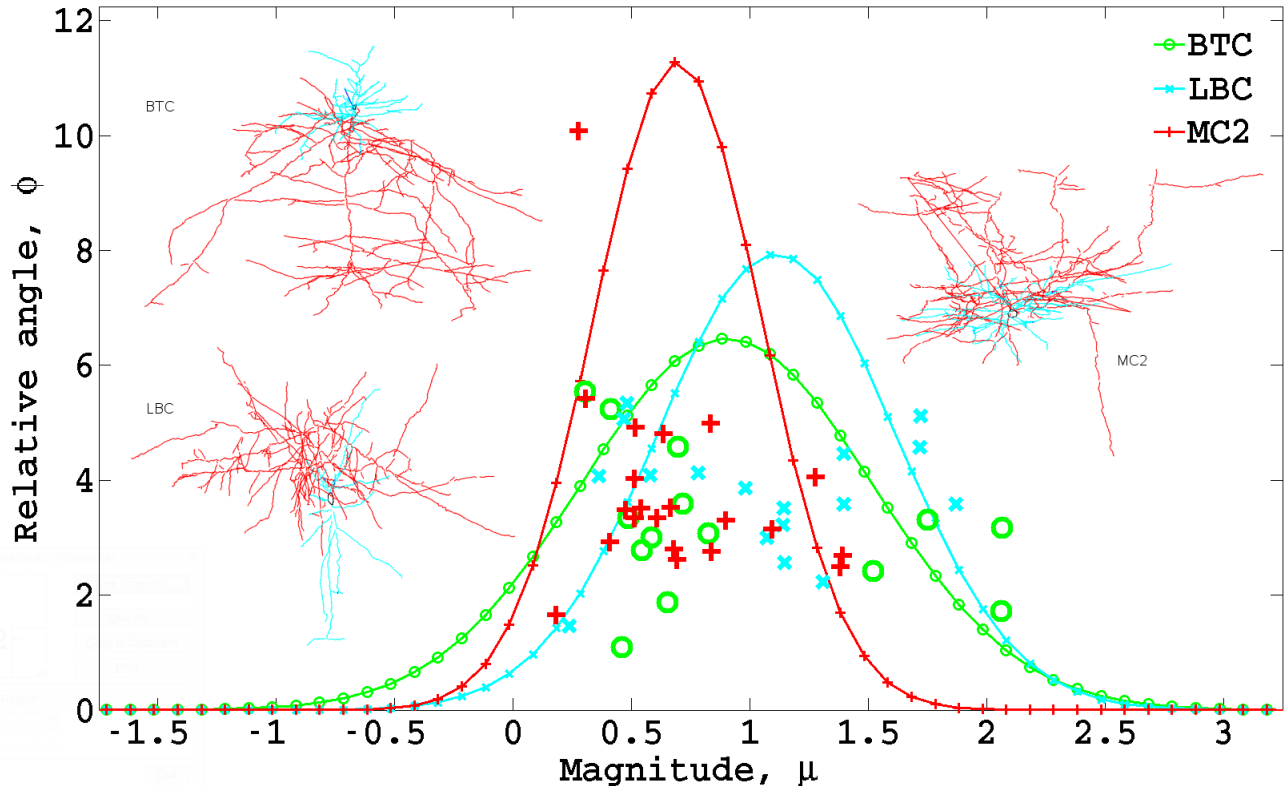


FIG. 1: The distribution of axonal-dendritic similarity among cells in the three neuronal classes.

sian fit. Recall that total morphologic similarity between the axonal and dendritic trees for each cell would result in a magnitude of difference vector equal to zero. The scatterplot in Figure 1 shows that most cells resulted with magnitude between 0 and 2 and angle between 0 and 6, with an outlier with angle near to 10 in the case of the MC2 cell category. As shown by the respective densities, the three classes of neuronal cells resulted with distinct dispersions, with the MC2 class being characterized by the smallest variance while the BTC class shows the largest variance. In order to obtain a more objective indication of the separation between the three neuronal cell categories, we performed the ANOVA variance test (e.g. [12]) and obtained the results (p -values) shown in Table II. These values indicate that the MC2 and LBC classes are those less likely to have come from the same population of cells, with a respective p -value of only 0.0088. Substantially higher values were obtained for the other pairs of categories, suggesting less separability in those cases.

Figure 1 also shows an example of neuronal cell for each of the anatomical classes, lying close to the center of the respective Gaussian distribution fit. Despite the difficulty of comparing the original 3D axonal and dendritic arborizations from such 2D projections, the larger difference between the two arborizations obtained in the

Class	BTC	LBC	MC2
BTC		0.2676	0.1629
LBC			0.0088
MC2			

TABLE II: The resulting p -values obtained through ANOVA for the 3 classes of neurons.

case of the LBC category is still clear, as well as the greater similarity observed for the MC2 cell example.

The obtained results suggest varying degrees of morphological relationship between the axonal and dendritic arborizations among all the considered individual cells and also between the three classes BTC, LBC and MC2. In the latter case, the classes LBC e MC2 resulted as being strongly statistically distinct. In brief, the methodology reported in this work has been found to provide a sensitive means for inferring differences between the axonal and dendritic structures. This is a particularly important result, as such differences may be related to important differentiation factors during the neuronal growth, including those caused by genetic modifications (cell predestination), environmental constraints (e.g., interactions with other cells and target specificity), as well

as the history of presented stimuli. The identification of such differences also present potential as a complementary subsidy for neuronal cell classification and diagnosis of abnormalities in neurological diseases, which correspond to interesting topics for further research.

Acknowledgments

Luciano da F. Costa is grateful to FAPESP (05/00587-5) and CNPq (308231/03-1) for financial support. Mar-

coni S. Barbosa is grateful to FAPESP (02/02504-1,03/02789-9) for sponsoring his post-doc programme.

-
- [1] L. da F. Costa. Morphological complex networks: Can individual morphology determine the general connectivity and dynamics of networks. *q-bio.MN/0503041*, 2001.
 - [2] H. B M Uylings and J. van Pelt. Measures for quantifying dendritic arborizations. *Network: Comput. Neural Syst.*, 13:397–414, 2002.
 - [3] R. Scorcioni, M. Lazarewicz, and G. Ascoli. Quantitative morphometry of hippocampal pyramidal cells: differences between anatomical classes and reconstructing laboratories. *J. Comp. Neurol*, 473:177–193, 2004.
 - [4] D. H. Sanes, T. A. Reh, and W. A. Harris. *Development of the nervous system*. Academic Press, 2005.
 - [5] H. Cline. Dendritic arbor development and synaptogenesis. *Current Opinion in Neurobiology*, 11:118–126, 2001.
 - [6] G. Kiddie, D. Mclean, A. V. Ooyen, and B. Graha. Biologically plausible models of neurite outgrowth. *Progress in Brain Research*, 147, 2005.
 - [7] K. Michelsen and H. de Raedt. Integral-geometry morphological image analysis. *Physics Report*, 347:461–538, 2001.
 - [8] M. S. Barbosa, E. S. Bernardes, and L. da F. Costa. Neuromorphometric characterisation with shape functionals. *Physical Review E*, 67(061910), 2003.
 - [9] M. S. Barbosa, L. da F. Costa, et al. Characterizing neuromorphological alterations with additive shape functionals. *European Physical Journal B*, 37:109–115, 2003.
 - [10] H. Markram. The blue brain project. *Nature Reviews, Neuroscience*, 7:153–160, 2006. Perspectives.
 - [11] H. Markram. Neocortical microcircuit database. <http://microcircuit.epfl.ch/>.
 - [12] R. V. Hogg and J. Ledolter. *Engineering Statistics*. MacMillan Publishing Company, 1987.